PHYSICS REPORTS (Review Section of Physics Letters) 219, Nos. 3–6 (1992) 243–262. North-Holland

PHYSICS REPORTS

Theoretical developments in cavity quantum optics: a brief review

Pierre Meystre

Optical Sciences Center and Department of Physics, University of Arizona, Tucson, AZ 85721, USA

Abstract:

We review some recent developments in theoretical cavity quantum optics, with special attention to the microwave regime and to aspects related to quantum measurement theory.

1. Introduction

This article reviews some recent developments in theoretical cavity quantum optics. We concentrate mostly on the microwave regime, where exceedingly high Q-factors can be achieved and the resonator can be thought of as a "photon trap", and specially address questions related to the quantum theory of measurement. Unfortunately, this does not allow us to do full justice to the spectacular progress recently witnessed in the optical regime of cavity quantum optics and to the considerable work that has been carried out in ion and neutral atom traps. Even within this restricted framework, it is impossible to give a complete review of the recent developments of the field within a few pages. We do not address the problem of radiative corrections in cavity QED, which is discussed in detail in two recent reviews by Haroche [1991] and Meschede [1992] and concentrate almost entirely on the so-called strong-coupling regime, characterized by spontaneous emission in the form of a nearly periodic exchange of energy between the atom and a cavity mode.

This paper, which is essentially an abridged version of a recent review [Meystre 1992], is organized as follows: In section 2, we outline important aspects of the Jaynes–Cummings model describing the dipole interaction between a single two-level atom and a single mode of the electromagnetic field. Section 3 outlines the concepts of enhanced and inhibited emission in the Born–Markov regime, using a density of modes approach. The strong coupling regime is discussed in section 4, using a coupled-modes approach. Section 5 outlines key features of the micromaser theory. The analysis of selective measurements is covered in section 6, while QND measurements are discussed in section 7. Section 8 then presents two proposed ways to generate Schrödinger cats in micromasers. Finally, section 9 is an outlook and conclusion.

Considerably more details and complete lists of references can be found in the recent reviews by Haroche [1992], Meschede [1992], and Meystre [1992]. The paper by Walther in this issue deals with experimental aspects of cavity QED. The contribution by Haroche extends our discussion of Schrödinger cats, while the paper by Kimble presents exciting recent results in the optical regime.

2. Jaynes–Cummings model

The simplest form of interaction between a two-level atom and a single quantized mode of the

electromagnetic field is described by the Jaynes–Cummings Hamiltonian [Jaynes and Cummings 1963, Barnett et al. 1986]

$$\mathscr{H} = \tfrac{1}{2}\hbar\omega\sigma_z + \hbar\Omega a^\dagger a + \hbar(ga^\dagger\sigma_- + \text{adj.}) = \mathscr{H}_0 + \mathscr{V}\,, \tag{2.1}$$

where

$$\mathscr{H}_0 = \tfrac{1}{2}\hbar\omega\sigma_z + \hbar\Omega a^\dagger a\,, \tag{2.2}$$

$$\mathscr{V} = \hbar(ga^\dagger\sigma_- + \text{adj.})\,. \tag{2.3}$$

Here, ω is the atomic transition frequency, Ω the field frequency, a and $a^\dagger$ are the boson annihilation and creation operators of the field mode, with $[a, a^\dagger] = 1$, σ_z, σ_- and σ_+ are atomic pseudo-spin operators, with $[\sigma_+, \sigma_-] = \sigma_z$. The coupling constant

$$g = (\mathscr{P}\mathscr{E}_\Omega/2\hbar)\sin KZ \tag{2.4}$$

is the electric dipole matrix element at the location Z of the atom, where $\mathscr{E}_\Omega$ is the "electric field per photon" $\mathscr{E}_\Omega = (\hbar\Omega/\varepsilon_0 V)^{1/2}$ [e.g. Meystre and Sargent 1991].

With the development of micromasers [Meschede, Walther and Müller 1985], it has become possible to reach experimental situations very close to a practical realization of this model and to investigate in detail the complexities of the atom–field dynamics in that simplest of all situations.

The eigenenergies of the Jaynes–Cummings Hamiltonian (2.1) are

$$E_{1n} = \hbar(n + \tfrac{1}{2})\Omega + \tfrac{1}{2}\hbar\mathscr{R}_n = \hbar[-\tfrac{1}{2}\omega + (n+1)\Omega + \tfrac{1}{2}(\mathscr{R}_n + \delta)]\,, \tag{2.5}$$

$$E_{2n} = \hbar(n + \tfrac{1}{2})\Omega - \tfrac{1}{2}\hbar\mathscr{R}_n = \hbar[\tfrac{1}{2}\omega + n\Omega - \tfrac{1}{2}(\mathscr{R}_n + \delta)]\,, \tag{2.6}$$

where $\delta = \omega - \Omega$ is the atom–field frequency detuning and we have introduced the generalized n-photon Rabi flopping frequency

$$\mathscr{R}_n = \sqrt{\delta^2 + 4g^2(n+1)}\,. \tag{2.7}$$

The corresponding eigenvectors are

$$|1, n\rangle = \sin\theta_n\,|\mathrm{a}, n\rangle + \cos\theta_n\,|\mathrm{b}, n+1\rangle\,, \tag{2.8}$$

$$|2, n\rangle = \cos\theta_n\,|\mathrm{a}, n\rangle - \sin\theta_n\,|\mathrm{b}, n+1\rangle\,, \tag{2.9}$$

where the state $|\mathrm{a}\rangle$ and $|\mathrm{b}\rangle$ are the upper and lower atomic states, respectively, and $|n\rangle$ are number states of the field mode with $a^\dagger a|n\rangle = n|n\rangle$. The angle θ is defined via the relations

$$\cos\theta_n = (\mathscr{R}_n - \delta)/\sqrt{(\mathscr{R}_n - \delta)^2 + 4g^2(n+1)}\,, \tag{2.10}$$

$$\sin\theta_n = 2g\sqrt{n+1}/\sqrt{(\mathscr{R}_n - \delta)^2 + 4g^2(n+1)}\,. \tag{2.11}$$

For $n = 0$ and on resonance $\omega = \Omega$, the dressed levels $|1,0\rangle$ and $|2,0\rangle$ are separated by the frequency

$$\mathcal{R}_0 = 2g\,, \tag{2.12}$$

the so-called vacuum Rabi splitting frequency.

From these results, it is possible to compute all dynamical properties of the Jaynes–Cummings model. In particular, assuming that the atom is initially in its upper state $|a\rangle$ and the field in the number state $|n\rangle$, we find that on resonance $\omega = \Omega$, the probability $|C_{an}(t)|^2$ for the atom to be in the upper state at time t is given by

$$|C_{an}(t)|^2 = \cos^2(g\sqrt{n+1}\,t)\,. \tag{2.13}$$

Similarly, if the atom is initially in its lower state $|b\rangle$, we find

$$|C_{an}(t)|^2 = \sin^2(g\sqrt{n}\,t)\,. \tag{2.14}$$

These results indicate that the upper state population oscillates periodically at the Rabi frequency, very much like in the case of classical fields. There is however an important difference between the two situations: in the case of a quantized field the Rabi frequency is different if the atom starts in the upper or the lower state, respectively. This is due to the non-commuting character of the creation and annihilation operators $a^\dagger$ and a.

The Rabi solutions (2.13) and (2.14) yield the simplest form of "spontaneous emission", as can be seen readily by setting $n = 0$ in these equations. For an atom initially in the upper state, this gives

$$|C_{a0}(t)|^2 = \cos^2(gt)\,, \tag{2.15}$$

while for an atom initially in its lower state we find

$$|C_{a0}(t)|^2 = 0\,. \tag{2.16}$$

In contrast, in the case of an atom driven by a classical field of zero amplitude, one would have $|C_{a0}(t)|^2 = 0$. The reason for this fundamental difference between the quantum and classical descriptions of the field lies in the fact that even though the expectation value of the quantized field amplitude vanishes, that for its intensity does not:

$$\langle E^2\rangle = \mathcal{E}_\Omega^2 \langle 0|(a + a^\dagger)^2|0\rangle = \mathcal{E}_\Omega^2\,. \tag{2.17}$$

Stated another way, the vacuum fluctuations effectively stimulate the excited atom to emit, a process called spontaneous emission. The slow Rabi flopping that occurs for $n = 0$ is due to spontaneous emission followed by reabsorption, a process which is neglected in the semiclassical approximation.

A number of further features of the Jaynes–Cummings model, including collapse [Cummings 1965] and revivals, are reviewed e.g. in [Barnett et al. 1986]. Revivals similar to the Jaynes-Cummings revivals [Eberly, Narozhny and Sanchez-Mondragon 1980] have been observed in a micromaser experiment by Rempe, Walther and Klein [1987].

3. Enhanced and inhibited spontaneous emission

The Jaynes–Cummings model exhibits a skeletal form of spontaneous emission whose signature is a periodic exchange of energy between the two-level atom and the initially empty cavity mode. In free space, the situation is completely different, as the atom interacts with a continuum of modes of the electromagnetic field. In this case, the probability amplitudes corresponding to the interaction of the atom with each of these modes interfere with one another and can lead to an exponential decay of the upper state population.

To treat this problem, we consider a two-level atom interacting with a multimode electromagnetic field. In the dipole and rotating-wave approximations, this interaction is described by the Hamiltonian

$$\mathscr{H}_{mm} = \tfrac{1}{2}\hbar\omega\sigma_z + \hbar\sum_s \Omega_s a_s^\dagger a_s + \hbar\sum_s (g_s a_s^\dagger \sigma_- + \text{adj.}) . \tag{3.1}$$

Here, Ω_s is the frequency of the sth mode of the field, a_s and $a_s^\dagger$ are the corresponding boson annihilation and creation operators, with $[a_s, a_{s'}^\dagger] = \delta_{s,s'}$, and g_s is the dipole coupling constant between the atom and mode s.

If the atom is initially in its upper state $|\mathrm{a}\rangle$ and the field in the multimode vacuum state $|\{0\}\rangle$, one easily finds that the probability $C_{\mathrm{a},\{0\}}$ for the atom to still be excited at time t is governed by the integro-differential equation [see e.g. Meystre and Sargent 1991]

$$\frac{\mathrm{d}}{\mathrm{d}t} C_{\mathrm{a},\{0\}} = -\sum_s |g_s|^2 \int_0^t \mathrm{d}t'\, C_{\mathrm{a},\{0\}}(t') \exp[\mathrm{i}(\Omega_s - \omega)(t - t')] . \tag{3.2}$$

This equation was first solved by Weisskopf and Wigner [1930], who found that in free space and in the so-called Born–Markov approximation, the upper state population decays exponentially at the rate

$$\gamma_{\mathrm{f}} = (1/4\pi\varepsilon_0)4\omega^3|d|^2/3\hbar c^3 , \tag{3.3}$$

where d is the dipole matrix element of the transition. The Weisskopf–Wigner theory predicts an *irreversible* exponential decay of the upper state population with no revivals and/or periodic exchange of energy between the atom and the field. Although under the action of each individual mode the atom would have a finite probability to return to its upper state, as in the Jaynes–Cummings problem, the probability amplitudes for all such events interfere destructively when summed over the continuum of free space modes.

The Weisskopf–Wigner decay rate γ_{f} depends explicitly on the density of modes of the electromagnetic field, as readily seen from eq. (3.2). Indeed, the result (3.3) is valid for free space only, as it replaces the sum in eq. (3.2) by an integral, where the measure is the free space mode density

$$\mathscr{D}_{\mathrm{f}}(\Omega) = \Omega^2/\pi^2 c^3 . \tag{3.4}$$

We also note that the Born–Markov approximation used in this derivation implicitly assumes a *weak coupling* between the atom and the electromagnetic field. Indeed, it results from successive applications of second-order perturbation theory and decorrelations of the atom from the field modes. Clearly, the Jaynes–Cummings result does not make this assumption and is valid to all orders. More generally, the

coupled-modes approach of section 4 will consider spontaneous emission of an atom in a cavity, and show that three different coupling constants must be considered and compared, g being one of them. In the *strong coupling limit* where g is the largest of these constants, spontaneous emission is qualitatively as well as quantitatively different from its weak coupling limit.

Concentrating for now on the weak coupling limit, and considering a geometry characterized by a mode density $\mathscr{D}_g(\Omega)$, we obtain the decay rate

$$\gamma_g \approx [\mathscr{D}_g(\Omega)/\mathscr{D}_f(\Omega)]\gamma_f\,, \tag{3.5}$$

provided that the Markov–Born approximation is still applicable. Depending on the value of $\mathscr{D}_g(\Omega)$, eq. (3.5) leads to enhanced [Purcell 1946] or inhibited [Kleppner 1981] spontaneous emission.

It is perhaps useful at this point to make a comment about the dependence of the spontaneous emission rate on the cavity density of modes. The mode structure depends on the boundary conditions imposed by the cavity, and one might wonder how the atom can initially "know" that it is inside a cavity rather than in free space. Is there some action at a distance involved, and if not, what is the mechanism through which the atom learns of its environment? This problem has been addressed by Parker and Stroud [1987] and by Cook and Milonni [1987]. These authors showed that a proper multimode description yields a simple answer to this question. In a real cavity, the atom initially in its upper state starts to spontaneously decay while radiating a multimode field that propagates away from the source. Eventually, this field encounters the cavity walls, which reflect it. The reflected field acts back on the atom, carrying information about the cavity walls as well as about the state of the atom itself at earlier times. If the phase of this field is just right, it will then prevent any further atomic decay. An alternative way to think of this problem, first discussed by Milonni and Knight [1973] is the image method that replaces the mirror cavity by a string of virtual images. This method, which is valid for cavities of dimensions $L \ll c/\gamma_f$, leads to the same results as the mode expansion results.

When the cavity Q becomes very high, the cavity damping rate ceases to dominate the atomic dynamics: the atom–field coupling constant g becomes the largest coupling constant and the Born–Markov approximation ceases to be valid. In this case, a more useful way to think of the problem is to consider the coupling of the atom to a single mode of the field selected by the cavity, this mode being in turn weakly coupled to a Markovian reservoir. The response function of the cavity has a finite bandwidth, and it passes a filtered version of the vacuum fluctuations to the atom, which therefore sees them as a "colored" reservoir. As far as spontaneous emission is concerned, the irreversible decay is now modulated by a periodic exchange of energy between the atom and the cavity mode.

For extreme Q's, one reaches a regime where spontaneous emission ceases to be irreversible. As $Q \to \infty$ one approaches the situation where the Jaynes–Cummings description of the atom–field system becomes appropriate and where spontaneous emission is in the form of a perfectly periodic exchange of energy between the atom and that field mode that is closest to resonance with the atomic transition.

4. Coupled-modes approach

We have seen in section 2 that the coupling of a single atom with a cavity mode in the vacuum state leads to the vacuum Rabi splitting (2.12). However, this simple argument assumes that both the cavity and the atom have infinitely narrow widths. As a result, it is impossible to determine if the splitting will be observable in practice or will be masked by the broadening mechanisms associated with losses.

We have also mentioned that the Weisskopf–Wigner theory of section 3 is inadequate in the strong coupling limit, as it implicitly assumes that the electric dipole coupling constant is small compared to the spontaneous decay rate γ and, in a cavity, to the cavity damping rate κ. For the closed cavities used in microwave experiments, these are the only relevant rates, and with Rydberg atoms, it is easy to reach both the weak coupling (or "bad cavity") regime $g \ll \kappa$ and the strong coupling (or "good cavity") regime $g \gg \kappa$. In contrast, the dynamics of an atom inside an open-sided optical cavity is characterized in general by three coupling constants. They are the atom–field coupling constant g, the rate γ' of spontaneous emission into free space, and the cavity damping rate κ. Most optical cavities encompass only a small fraction of the free space 4π solid angle, so that $\gamma' \approx \gamma_f$, and the coherent coupling rate g is usually exceeded by κ and/or γ'. Fortunately, the collective enhancement of $g \to g_{\text{eff}} = g\sqrt{N}$ that occurs for N atoms inside a wavelength [Haroche and Raimond 1985] offers a way out of this difficulty and permits to perform experiments in the strong coupling regime $g_{\text{eff}} \gg \gamma > \kappa$ [Raizen et al. 1989]. This multi-atom enhancement has been employed successfully to observe the vacuum Rabi splitting in the optical regime [Kaluzny et al. 1983, Brecha et al. 1986, Raizen et al. 1989]. The strong coupling regime can also be reached by decreasing the volume of the cavity, thereby increasing the electric field per photon $\mathscr{E}_\Omega = (\hbar\Omega/\varepsilon_0 V)^{1/2}$ and hence the dipole coupling constant (2.4). This technique has recently been used by Kimble's group to observe absorptive optical bistability in the optical regime with as few as 10 atoms or so at a time in the cavity [Kimble 1990, see also Kimble's contribution in this issue].

The general situation where all three rates g, γ' and κ are important has been investigated mostly by the groups of Carmichael, Kimble and Savage. Theoretically, one considers a single two-level atom coupled to a single cavity mode (note that this is different from the degenerate modes situation studied by Heinzen et al. [1987]). The cavity mode is in turn coupled to a reservoir that accounts for cavity losses, while the atom is coupled to the free space modes not encompassed by the cavity, leading to a spontaneous decay rate γ'. The interaction between the atom and a single cavity mode can be modeled by the master equation [Carmichael et al. 1989, Savage 1990]

$$\dot{\rho} = (1/\mathrm{i}\hbar)[\mathscr{V}, \rho] + \tfrac{1}{2}\gamma'(2\sigma_-\rho\sigma_+ - \sigma_+\sigma_-\rho - \rho\sigma_+\sigma_-) + \kappa(2a\rho a^\dagger - a^\dagger a\rho - \rho a^\dagger a)\,, \tag{4.1}$$

where ρ is the atom–cavity mode density matrix, 2κ is the photon decay rate of the cavity, and $\mathscr{V}$ is given by eq. (2.3).

To describe spontaneous emission for arbitrary values of γ', κ and g_{eff}, we solve the master equation (4.1) in the three-state basis $|a, 0\rangle$, $|b, 1\rangle$ and $|b, 0\rangle$, where $|0\rangle$ and $|1\rangle$ are the zero- and one-photon Fock states of the field. In this basis, ρ has eight independent matrix elements. Writing the master equation (4.1) formally as

$$\dot{\rho} = (1/\mathrm{i}\hbar)[\mathscr{V}, \rho] + L\rho\,, \tag{4.2}$$

the evolution of the expectation value of an operator O is given by

$$\frac{\mathrm{d}}{\mathrm{d}t}\langle O\rangle = (1/\mathrm{i}\hbar)\langle[O, \mathscr{V}]\rangle + \mathrm{Tr}(OL\rho) \tag{4.3}$$

and we obtain readily the two sets of coupled equations [Carmichael et al. 1989]

$$\langle \dot{a}\rangle = -\mathrm{i}g\langle\sigma_-\rangle - \kappa\langle a\rangle\,, \tag{4.4}$$

$$\langle \dot{\sigma}_- \rangle = -ig\langle a \rangle - \gamma'/2\langle \sigma_- \rangle \tag{4.5}$$

and

$$(d/dt)\langle a^\dagger a \rangle = ig(\langle a^\dagger \sigma_- \rangle - \langle a\sigma_+ \rangle) - 2\kappa\langle a^\dagger a \rangle , \tag{4.6}$$

$$(d/dt)\langle \sigma_+ \sigma_- \rangle = ig(\langle a^\dagger \sigma_- \rangle - \langle a\sigma_+ \rangle) - \gamma'\langle \sigma_+ \sigma_- \rangle , \tag{4.7}$$

$$(d/dt)\langle a^\dagger \sigma_- \rangle = -g(\langle a^\dagger a \rangle - \langle \sigma_+ \sigma_- \rangle) - (\kappa + \tfrac{1}{2}\gamma')\langle a^\dagger \sigma_- \rangle . \tag{4.8}$$

Equations (4.4) and (4.5) describe the decay of the amplitudes of two coupled harmonic amplitudes. Specifically, if the atom–field system is prepared in the state $a|a,0\rangle + b_0|b,0\rangle + b_1|b,1\rangle$, where a, b_0 and b_1 are real constants, then eqs. (4.4) and (4.5) describe the decay of the mean field and atomic polarization amplitudes. In the strong coupling limit $g \gg \kappa$, γ', the mean "energy" $\langle a^2 \rangle + \langle \sigma_- \rangle^2$ oscillates between the atom and the field as it decays. In the limiting case $\kappa = 0$, and for the initial condition $\langle a \rangle = 0$, $\langle \sigma_- \rangle = ab_0$, we have

$$E = (ab_0)^2 \exp(-\gamma' t/2)[1 - (\gamma'/4g)\sin(2gt)] , \tag{4.9}$$

that is, E decays at the average rate $(2\kappa + \gamma')/2 = \gamma'/2$. The reason for the average between the atomic and cavity decay rates is revealed by the decay rate $-\dot{E}/E = \frac{1}{2}\gamma'[1 + \cos(2gt)]$, which oscillates between the maximum of γ' and the minimum value of 0 $(=2\kappa)$, so that the decay rate is averaged as the energy oscillates between the polarization and the field [Carmichael et al. 1989].

In this regime, the spontaneous emission spectrum splits into two lines which correspond precisely to the normal-mode splitting of coupled harmonic oscillators. Specifically, the spontaneous emission spectrum $S(\omega)$ is given by the doublet

$$2\pi S(\omega) = \frac{\kappa/2 + \gamma'/4}{(\kappa/2 + \gamma'/4)^2 + (\Omega - \omega - g)^2} + \frac{\kappa/2 + \gamma'/4}{(\kappa/2 + \gamma'/4)^2 + (\Omega - \omega + g)^2} . \tag{4.10}$$

It consists of two peaks separated by the vacuum Rabi frequency $2g$ (see eq. (2.12)) and their half linewidth $(\kappa + \gamma')/2$ is less than the free space linewidth whenever $\kappa < \gamma'/2$.

In the "bad cavity" limit $\kappa \gg g \gg \gamma'/2$, in contrast, the spontaneous emission spectrum reduces to a conventional single-peak Lorentzian

$$2\pi S(\omega) = \frac{\gamma' + 2g^2/\kappa}{(\gamma'/2 + g^2/\kappa)^2 + (\omega - \Omega)^2} \tag{4.11}$$

which exhibits the increased linewidth (enhanced spontaneous emission) discussed in section 3 [Carmichael et al. 1989].

The experimental verification of the strong-coupling prediction was performed by Raizen et al. [1989], who used the cooperative response of N two-level atoms in a high-finesse cavity to reach the condition $g_{\text{eff}} = g\sqrt{N} \gg \gamma' > \kappa$. These experiments verified that the transmission spectrum was split into a doublet separated by the vacuum Rabi frequency, and observed subnatural linewidth averaging, with linewidth reductions of 25% relative to the free-space atomic decay.

5. The micromaser

In this and the following sections, we specialize to cavity quantum optics in the microwave regime, and in particular to the micromaser. This work is characterized by the use of closed superconducting cavities with exceedingly small losses, so that $\gamma' \approx 0$ and the strong coupling limit $g \gg \kappa, \gamma'$ is realized. In general, the calculation of the modes structure of these cavities near the cut-off frequency is complicated, although explicit calculations have been performed by Baltes, Muri and Kneubühl [1970] and by Baltes and Kneubühl [1972] (see also Baltes and Hilf [1976]) in connection with the theory and calibration of IR detectors. Fortunately, the two-level atoms used to pump the micromaser are typically resonant or near-resonant with one of these modes only, so that a single-mode description of the resonator is appropriate. In such situations, many of the results of the Jaynes–Cummings model still hold, and the dynamics of the system is characterized by a nearly periodic exchange of energy between the atom and the cavity mode [Rempe, Walther and Klein 1987].

Consider specifically the situation of a micromaser, which is a device where a low density beam of Rydberg atoms is injected inside a single mode microwave cavity at such a low rate that at most one atom at a time is present inside the resonator. Micromaser cavities are manufactured from pure niobium and cooled down to a fraction of a kelvin, thereby achieving quality factors Q up to 3×10^{10}. The Max-Planck Institute experiments [Meschede, Walther and Müller 1985] consider a micromaser operating on a single photon transition, while the Ecole Normale Superieure experiments [Brune et al. 1987] concentrate on two-photon micromasers.

Rydberg atoms have enormous electric dipole moments, scaling as the square of the principal quantum number n, so that the transition probability for single-photon induced transitions between closely adjacent levels scales as n^4. Their spontaneous lifetimes are also very large, scaling as n^3 and n^5 for low and high angular momentum states, respectively [Haroche 1982]. This implies that the saturation power fluxes for transitions between neighboring levels become extremely small. For instance, for $n = 30$ and low angular momentum states, 100 photons per squared wavelength are sufficient to saturate the transition, this number being reduced to 1 for high angular momentum transitions. The advantage of using Rydberg atoms is even more dramatic for two-photon transitions, as the two-photon coupling constant scales as n^4.

One "drawback" of performing experiments in the microwave regime is the lack of good photon detectors. To investigate the intracavity field, one studies instead the state of the Rydberg atoms as they exit the resonator. As such, the atoms play the dual role of pump and detectors. This detection scheme, which provides only indirect information on the state of the cavity field, makes the micromaser a particularly attractive test system to investigate a number of aspects of quantum measurement theory [Meystre 1987, Meystre and Wright 1988, Krause, Scully and Walther 1987].

Indeed, the interest in studying micromasers is manifold. In addition to the issues in quantum measurement theory just mentioned, they are theoretically attractive in that the amplifying medium is so simple that an accurate quantum treatment is possible [Filipowicz, Javanainen and Meystre 1986a, Lugiato, Scully and Walther 1987, Davidovich et al. 1987]. Furthermore, quantum fluctuations play a very important role in these systems, since the mean photon number in the cavity is extremely low. Moreover, micromasers can be operated in a regime where all causes of inhomogeneous line broadening have been eliminated and irreversible spontaneous emission can be ignored. Hence, the successive atoms undergo coherent, quantum Rabi oscillations as they interact with the cavity field. (To reach this regime, it is important to ensure that the interaction time of the successive atoms with the cavity mode is constant. This is achieved by passing the atomic beam through a Fizeau velocity selector.)

The quantum theory of the micromaser [Filipowicz, Javanainen and Meystre 1986a] relies on its unique characteristics: Firstly, because the atom-field interaction takes place in a closed, single-mode cavity, the spontaneous emission rate γ' into free-space modes can be neglected. Secondly, due to the extremely high quality factors achieved in these superconducting cavities, the photon lifetime is extremely long compared to the transit time τ of the successive atoms through the resonator. This means that cavity damping can practically be ignored while an atom interacts with the field [Barnett and Knight 1985, Nayak, Bullough and Thompson 1990]. Since the atomic flux needs to be kept small enough for at most one atom to be present inside the cavity at a time, the interval between atoms must be much larger than τ, and hence the cavity is empty most of the time, so that we neglect cavity damping only during these rare instances where an atom interacts with the cavity mode.

The strategy to theoretically describe the micromaser is then straightforward: while an atom is inside the cavity, the coupled atom-field system is described by the Jaynes–Cummings Hamiltonian (2.1), and during the intervals between atoms the evolution of the field density matrix ρ_f is governed by the master equation [Louisell 1990]

$$\mathrm{d}\rho_f/\mathrm{d}t \equiv L\rho_f(t_i) = \tfrac{1}{2}\kappa(n_b + 1)(2a\rho_f a^\dagger - a^\dagger a\rho_f - \rho_f a^\dagger a) + \tfrac{1}{2}\kappa n_b(2a^\dagger\rho_f a - aa^\dagger\rho_f - \rho_f aa^\dagger)\,, \tag{5.1}$$

where we have generalized the expression used in eq. (4.1) to include the mean number n_b of thermal photons present in the cavity mode.

At time t_i, the ith atom enters the cavity containing the field described by the density operator $\rho_f(t_i)$. At this time, the density operator $\rho(t_i)$ of the combined atom–field system is simply the tensor product of $\rho_f(t_i)$ and the initial atomic density operator. After the interaction time τ, the atom exits the resonator and leaves the field in the state described by the reduced density operator

$$\rho_f(t_i + \tau) = \mathrm{Tr}_a[U(\tau)\rho(t_i)U^\dagger(\tau)] \equiv F(\tau)\rho_f(t_i)\,, \tag{5.2}$$

where Tr_a stands for trace over the atomic variables. Note that this step *explicitly assumes that the state of the atom is not measured as it exits the cavity*. Otherwise, the theory has to be modified according to the discussion of the next section. Using eq. (5.1) for the field evolution during the interval t_p until the time t_{i+1} when the next atom is injected, and noting that $t_p = t_{i+1} - t_i - \tau \approx t_{i+1} - t_i$ we have then

$$\rho_f(t_{i+1}) = \exp(Lt_p)F(\tau)\rho_f(t_i)\,. \tag{5.3}$$

This equation can be further simplified by assuming that the atoms enter the cavity according to a Poisson process with mean spacing $1/R$ between events, where R is the atomic flux. Equation (5.3) reduces then to [Filipowicz, Javanainen and Meystre 1986a]

$$\bar{\rho}_f(t_{i+1}) = (1 - L/R)^{-1}F(\tau)\bar{\rho}_f(t_i)\,. \tag{5.4}$$

In steady state $\bar{\rho}_f(t_{i+1}) = \bar{\rho}_f(t_i) = \bar{\rho}_{f,st}$, and introducing the notation

$$N_{ex} = R/\kappa \tag{5.5}$$

for the average number of atoms that traverse the cavity during the resonator damping time, one finds the photon statistics

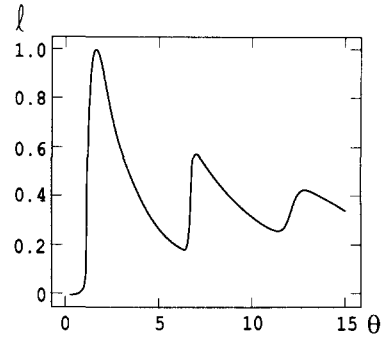

Fig. 1. Normalized steady-state mean photon number l as a function of the pump parameter Θ for $N_{ex} = 200$ and $n_b = 0.1$. (After Filipowicz, Javanainen and Meystre [1986a]).

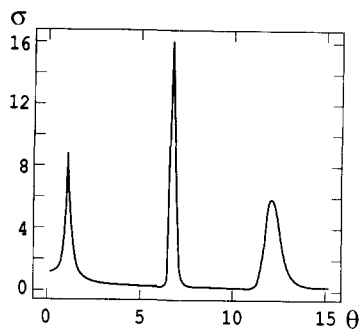

Fig. 2. Normalized standard deviation σ of the steady-state photon distribution for $N_{ex} = 200$ and $n_b = 0.1$. (After Filipowicz, Javanainen and Meystre [1986a]).

$$\rho_n = C\left(\frac{n_b}{1+n_b}\right)^n \prod_{k=1}^{n}\left(1+\frac{N_{ex}\sin^2 \mathcal{R}_k}{n_b k}\right). \tag{5.6}$$

Figure 1 shows the normalized average photon number $l = \langle n\rangle / N_{ex}$ as a function of the dimensionless pump parameter

$$\Theta = \sqrt{N_{ex}}\, g\tau \tag{5.7}$$

for various values of N_{ex} and for a mean thermal photon number $n_b = 0.1$. A common feature of all cases is that l is nearly zero for small Θ, but a finite value emerges at the threshold value $\Theta = 1$. For Θ increasing past this point, l grows rapidly, but then decreases to reach a minimum at $\Theta \approx 2\pi$, where the field jumps abruptly to a high intensity. This general behavior recurs roughly at integer multiples of 2π, but becomes less pronounced for increasing Θ.

As illustrated in fig. 2, similar thresholds are apparent in the behaviour of the normalized standard deviation

$$\sigma = [(\langle n^2\rangle - \langle n\rangle^2)/\langle n\rangle]^{1/2}, \tag{5.8}$$

where σ^2 is often called the Fano factor and $\sigma^2 - 1$ is the Mandel parameter. Above the threshold $\Theta = 1$ the photon statistics are first strongly superpoissonian (poissonian photon statistics correspond to $\sigma = 1$), with further superpoissonian peaks occurring for Θ roughly equal to multiples of 2π. In the remaining intervals of Θ, σ is typically of the order of 0.5, a signature of the subpoissonian nature of the field. Experiments verifying these unique features of micromasers, which result from the *coherent* nature of the atoms–field interaction, have been carried out by Meschede, Walther and Müller [1985], Rempe, Walther and Klein [1987] and Rempe, Schmidt-Kaler and Walther [1990].

6. Quantum measurements on the micromaser field

In its most widely accepted interpretation, quantum mechanics predicts the behaviour of an *ensemble* of identically prepared systems, and a naive use of the density matrix is not adequate to describe the

dynamics of a single quantum system. Instead, some conventional wisdom must be revised, and new quantum mechanical tools introduced to handle these situations. This has recently been realized by a number of authors, in particular in connection with the descriptions of "quantum jumps" of isolated ions and in micromasers [Dehmelt 1975, Cook and Kimble 1985, Nagourney, Sandberg and Dehmelt 1986, Javanainen 1986, Schenzle, deVoe and Brewer 1986, Cohen-Tannoudji and Dalibard 1986, Meystre 1987, Meystre and Wright 1988, Brune et al. 1990].

To properly describe the dynamics of single quantum systems, the measurements performed must be taken explicitly into account. This requires coupling the system under investigation to a meter system. The measurement process typically produces a back-action on the system and influences its subsequent dynamics. Thus, the observed dynamics are both measurements-induced and measurements-dependent. This is quite different from the classical situation, where any observation of the system would involve some intervention from the outside, but the structure of the theory is such that the effects of measurements can easily be ignored [Lamb 1985, 1986].

The micromaser represents an almost ideal test system to study the effects of repeated measurements on a single, isolated or nearly isolated quantum system. As the successive atoms used to pump the maser exit the cavity, their state can be measured, e.g. by the method of state-selective field ionization [Haroche and Raimond 1984, Meschede, Walther and Müller 1985, Rempe, Schmidt-Kaler and Walther 1990]. As such, the atoms play the dual role of pumps and detectors, and their final state is used to extract information about the state of the cavity mode. If we merely verify that the atoms exit the cavity as in the preceding section (so-called "non-selective measurements"), the micromaser normally reaches a unique steady state. In contrast, monitoring the state of the atoms as they exit the cavity ("selective measurements") typically leads to complex dynamics, such as e.g. quantum relaxation-oscillations and measurements-induced quantum diffusion [Meystre and Wright 1988].

To illustrate this discussion, we analyze repeated measurements on the field of a lossless micromaser [Meystre 1987]. Although this simplified model is only a caricature of the micromaser, it permits to explicitly discuss the essential steps required to describe the associated dynamics: preparation, Schrödinger evolution, measurement, reduction of the wave packet, and renormalization of the density matrix.

In the absence of cavity damping, the micromaser is described by the Jaynes–Cummings Hamiltonian (2.1) while an atom is inside the cavity and by a damped harmonic oscillator when no atom is present. We assume in the present discussion that the successive atoms are injected in their upper state and that the field density matrix is initially diagonal in the energy representation.

If no measurement is performed on the ith atom as it exits the cavity, or more precisely if we just make sure that it leaves the cavity at time $t_i + \tau$, then the reduced density matrix for the field alone is given by eq. (5.2). The corresponding photon statistics are

$$p_n(t_i + \tau) = p_{n-1}(t_i) \sin^2 \mathscr{R}_n \tau/2 + p_n(t_i) \cos^2 \mathscr{R}_{n+1} \tau/2 , \tag{6.1}$$

where $p_n(t_i)$ is the field photon statistics just before injection of the ith atom.

The results are quite different if a measurement of the state of the atom is performed as it exits the cavity. Specifically, if the atom is found in its state $|s\rangle$, where $s = \mathrm{a}, \mathrm{b}$ is either the upper or the lower state, the field density matrix after measurement becomes

$$\rho_f(t_i + \tau) = \mathrm{Tr}_a[|s\rangle\langle s|U(\tau)\rho(t_i)U^\dagger(\tau)] \tag{6.2}$$

with corresponding photon statistics

$$p_n^{\mathrm{a}}(t_i+\tau)=\mathcal{N}_{\mathrm{a}}p_n(t_i)\cos^2\mathcal{R}_{n+1}\tau/2 \tag{6.3}$$

or

$$p_n^{\mathrm{b}}(t_i+\tau)=\mathcal{N}_{\mathrm{b}}p_{n-1}(t_i)\sin^2\mathcal{R}_n\tau/2\,. \tag{6.4}$$

Here $\mathcal{N}_{\mathrm{a}}$ and $\mathcal{N}_{\mathrm{b}}$ are normalization constants that *must* be introduced to guarantee that the field density matrix remains normalized after the measurement.

Under the Jaynes–Cummings evolution, the probability that an atom initially in the excited state exits the cavity in that same state is given by

$$p_{\mathrm{a}}(t_i+\tau)=\sum_n p_n\cos^2\mathcal{R}_{n+1}\tau\,, \tag{6.5}$$

and the outcome of a given measurement will yield eqs. (6.3) or (6.4) with probabilities p_{a} and $1-p_{\mathrm{a}}$, respectively.

It is important to realize that measuring the atom in its upper state as it exits the resonator *does not* imply that the field, or even the mean photon number, remains unchanged. Rather, the photon statistics are reshuffled according to eq. (6.3), and the mean photon number $\langle n\rangle$ becomes

$$\sum_n np_n(t_i)\rightarrow\mathcal{N}_{\mathrm{a}}p_n(t_i)\cos^2\mathcal{R}_{n+1}\tau/2\,. \tag{6.6}$$

This result is not surprising: before the measurement, the mean photon number $\langle n\rangle$ is known only to within its standard deviation σ^2, and not conserving $\langle n\rangle$ does not violate any law of physics. It is only if the field happens to be in a number state $|n_0\rangle$, with $p_n=\delta_{n,n_0}$, at the time of injection of the ith atom, that the exact conservation of $\langle n\rangle$ is guaranteed when the atom exits the cavity in its upper state. Similar considerations apply if the atom exits in its lower state, and in this case, $\langle n\rangle$ can likewise either increase or decrease within the limits permitted by the variance of the photon statistics.

To numerically simulate a possible sequence of measurements, we can proceed by choosing an initial field density matrix, typically a thermal field with average photon number $\langle n_{\mathrm{b}}\rangle$, so that $p_n(0)=1/(1+n_{\mathrm{b}})[n_{\mathrm{b}}/(1+n_{\mathrm{b}})]^n$. This permits to compute from eq. (6.5) the probability p_{a} for the first atom to leave the cavity in the upper state. A random generator returns a uniform random variate r between 0 and 1. We say that the atom is measured in the upper state if $r>p_{\mathrm{a}}$ and in the lower state if $r<p_{\mathrm{a}}$. The field density matrix just after the measurement is completed is then given by either (6.3) or (6.4), depending on the outcome of the measurement. The same procedure is then repeated for the next atom, starting from this new field initial condition. Meystre [1987] shows how this procedure combined with the use of trapping states of the electromagnetic field [Filipowicz, Javanainen and Meystre 1986b], can be used to generate number states or mixtures of few number states of the electromagnetic field in a lossless micromaser (see also Meystre [1989]). Meystre and Wright [1989] have carried out a similar analysis to study the effects of measurements on the dynamics of a micromaser with damping. Alternative schemes using state reduction to generate number states in a micromaser cavity have also been proposed and analyzed by Krause, Scully and Walther [1987], Krause et al. [1989].

A description similar to that just given, but that does not make any assumption about the microscopic nature of the photodetector, was given by Srinivas and Davies [1981, 1982], and explicitly developed by Imoto, Haus and Yamamoto [1985], Imoto, Watkins and Sasaki [1987], Imoto and Saito [1989], Ueda [1989], Ueda, Imoto and Ogawa [1990], and Ogawa, Ueda and Imoto [1991] for the case of single-mode fields in a variety of initial states. In this model, it is assumed that the probability of more than one photon being detected during an infinitesimal time interval is negligible, and that the detector has unit quantum efficiency, so that the detection process can be decomposed into a sequence of "no-count processes" and "one-count processes".

7. QND measurements in micromaser cavities

Equation (6.6) clearly evidences the back-action of the measurements on the mean photon number $\langle n \rangle$. Recently, Brune et al. [1990] have proposed and analyzed a quantum non-demolition (QND) scheme [Braginsky, Vorontsov and Khalili 1977, Thorne et al. 1979, Caves 1983, Unruh 1987, Caves et al. 1980, Caves 1983] that permits to measure $\langle n \rangle$ in a back-action-evading manner. (For a review of QND in optical systems and a complete list of references, see the paper by Collett and Walls in this issue.) Their technique relies on the nonresonant coupling of the field to two-level atoms, and infers $\langle n \rangle$ by measuring the phase shift of the atomic wave-function at the exit of the resonator. Because of the strong atom–field coupling that can be achieved with Rydberg atoms, the proposed method presents the advantage of being applicable down to $\langle n \rangle \to 0$.

To understand how this technique works, consider a three-level Rydberg atom with levels $|\mathrm{a}\rangle$, $|\mathrm{b}\rangle$ and $|\mathrm{i}\rangle$, where $|\mathrm{a}\rangle$ and $|\mathrm{b}\rangle$ label the upper and lower levels as before and $|\mathrm{i}\rangle$ labels an intermediate level which can be reached from level $|\mathrm{a}\rangle$ by absorption of one photon. We assume the frequency Ω of the cavity mode under consideration to be nearly resonant with the transition frequency between the excited and intermediate levels, with detuning

$$\delta = \omega_{\mathrm{ia}} - \Omega \,. \tag{7.1}$$

From eqs. (2.5) and (2.6), we find readily that for an intracavity field in the Fock state $|n\rangle$, the upper level $|\mathrm{a}\rangle$ undergoes a dynamic Stark shift. Subtracting the bare energies of the uncoupled atom–field system from the corresponding dressed energies we find

$$\Delta(\boldsymbol{r}, n) = \tfrac{1}{2}(\mathscr{R}_{n-1} - \delta) = \tfrac{1}{2}[\sqrt{\delta^2 + 4d^2(\boldsymbol{r})n} - \delta] \,, \tag{7.2}$$

where we have slightly generalized the form of the Rabi frequency to allow for a spatially dependent atom field coupling constant, that we call d instead of g to avoid confusion between the $|\mathrm{a}\rangle \to |\mathrm{b}\rangle$ and the $|\mathrm{a}\rangle \to |\mathrm{i}\rangle$ transition. For sufficiently large detunings, this expression can be expanded to give

$$\Delta(\boldsymbol{r}, n) = d^2(\boldsymbol{r})n/\delta \,. \tag{7.3}$$

We see, then, that the Stark shift experienced by the excited state with respect to the ground state is proportional to the photon number in the cavity. (The ground state is not notably shifted if $\Omega - \omega_{\mathrm{ab}}$ is much larger than δ.) The accumulated phase-shift per photon is $\langle \Delta(\boldsymbol{r}, n = 1) \rangle L_{\mathrm{c}}/v_0$ where $\langle\ \rangle$ denotes a spatial average along the atom path through the cavity. Large single-photon shifts can be obtained by

choosing detunings δ that are relatively small, yet large enough that no significant absorption takes place.

The shift (7.3) alters the probability amplitude for the atom to be in the excited state $|a\rangle$ relative to that for being in the ground state, a change that can be detected by a phase-sensitive measurement. The setup of the proposed experiment is based on Ramsey's method of separated fields [Ramsey 1985]. The micromaser cavity is placed between two field zones R_1 and R_2 driving the $|a\rangle$–$|b\rangle$ transition. This transition is then detected behind R_2 by state-selective field ionization.

Consider an atom moving at the nominal velocity v_0 across the length L_c of the cavity. In the absence of signal field, the phase shift between the atom and the Ramsey field reference is

$$\phi_0 = (\Omega_r - \omega_{ab}) L_c / v_0 , \tag{7.4}$$

where Ω_r is the frequency of the fields R_1 and R_2. Assuming that each Ramsey field acts as a $\pi/2$ pulse on the atomic transition $|a\rangle$–$|b\rangle$ for atoms moving at the nominal velocity v_0, then the probability that atoms at velocity v exit the second Ramsey field in the excited state is

$$P_a(v, 0) = \sin^2(\pi v_0 / 2v) \cos^2(\phi_0 v_0 / 2v) , \tag{7.5}$$

while in the presence of (exactly) n photons in the cavity it becomes

$$P_a(v, n) = \sin^2(\pi v_0 / 2v) \cos^2[(\phi_0 - n\varepsilon) v_0 / 2v] , \tag{7.6}$$

that is, the Ramsey fringes are shifted by an amount $n\varepsilon$ with respect to their position when the cavity is empty. In practice, the atomic response must be averaged over the atomic velocity distribution $\mathcal{D}(v)$ and the field photon statistics $p(N)$.

We assume that the field is initially described by the photon statistics $p_0(N)$ and perform the analysis of a sequence of experiments along lines following exactly the discussion of the preceding section. Depending upon whether the first atom is measured in the upper or the lower state, the field density operator is "reduced" to

$$p_1(N) = p_0(N) \mathcal{P}(a, v_1, N) \Big/ \sum_M p_0(M) \mathcal{P}(a, v_1, M) \tag{7.7}$$

or

$$p_1(N) = p_0(N) \mathcal{P}(b, v_1, N) \Big/ \sum_M p_0(M) \mathcal{P}(b, v_1, M) \tag{7.8}$$

where $\mathcal{P}(b, v_1, n)$ is the probability that an atom at velocity v_1 and interacting with the Fock state $|n\rangle$ exits the cavity in the upper state. Assuming that a sequence of N measurements yields as a result the sequence $\{s_k, v_k\}$, by which we mean that the atom used for the kth measurement has velocity v_k and exits the second Ramsey field in the state $|s\rangle$ (s = a or b), we find the conditional probability of having n photons in the field as

$$p_n(N) = p_0(N) \prod_k \mathcal{P}(s_k, v_k, N) \Big/ \sum_M p_0(M) \prod_k \mathcal{P}(s_k, v_k, M) . \tag{7.9}$$

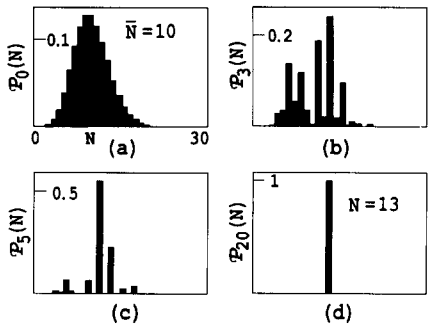

Fig. 3. Evolution of the photon number distribution p_n^N in a simulation of a measuring sequence. (a) Initial distribution (coherent state with a mean photon number $\bar{n} = 10$; (b)–(d) photon statistics after 3, 5 and 20 detected atoms. The collapse into a Fock state is clearly observable (after Brune et al. [1990]).

Figure 3 shows the result of a numerical simulation of such a measurement sequence. This simulation is carried out very much in the same way as the simulations discussed in section 6, except that a supplementary random number must be chosen to select the velocity of the kth atom. Quite generally, Brune et al. [1990] note that $p_n(N)$ converges to the Kronecker delta function representing a Fock state somewhere within the width of the original distribution. This "collapse" requires a certain number of atoms (about 20 for the example of the figure) which these authors call an "elementary measuring sequence". This shows that a single atom is not sufficient to provide a complete measurement of n, which is "pinned down" to a precise value only by gathering enough information through repeated atom detections. Each one results in multiplying the photon statistics p_n by a function of n presenting peaks and minima, thus decimating efficiently some photon numbers in the distribution, until only one is left. From then on the field statistics cannot change any longer, and a number state has been effectively prepared and can be repeatedly measured. Note that contrary to the situation encountered in the resonant detection schemes, undetected atoms do not change the photon statistics here.

The argument leading to eq. (7.9) does not include field dissipation between atoms. For weak enough losses, this problem can be treated along the lines of micromaser theory, neglecting dissipation while atoms are inside the cavity [Filipowicz et al. 1986a]. Brune et al. [1990] performed such simulations, and were able to demonstrate "quantum jumps" of the field as its energy is dissipated.

8. Macroscopic superpositions

The generation of macroscopic quantum superpositions is a question of considerable importance in the study of the relationship between quantum and classical physics [Leggett 1980]. While evidence for quantum tunneling has been established [Martinis, Devoret and Clarke 1988], the observation of quantum coherences is more difficult. A major problem is that macroscopic objects are not isolated but are coupled to their environment, which causes quantum coherences to be destroyed on a very fast time scale. Examples showing the influence of dissipation on macroscopic superpositions and the concomitant destruction of quantum-mechanical interference phenomena have been discussed by Caldeira and Leggett [1985], Walls and Milburn [1985] and Savage and Walls [1985].

Optically, a method to generate a superposition of macroscopically separated quantum states by propagating a coherent state through a Kerr nonlinear medium has been proposed by Yurke and Stoler

[1986], but this scheme suffers the same difficulties with dissipation. From this point of view, cavity QED experiments in the microwave regime, with the associated high-Q resonators, provide an interesting alternative. Two explicit schemes have been discussed by Slosser and co-workers [Slosser, Meystre and Braunstein 1989, Slosser, Meystre and Wright 1990, Meystre, Slosser and Wilkens 1990], and by Brune et al. [1992]. Both methods rely on injecting a monokinetic beam of polarized atoms, i.e. atoms prepared in the coherent superposition

$$|\psi\rangle = \alpha|\mathrm{a}\rangle + \beta|\mathrm{b}\rangle \tag{8.1}$$

inside a micromaser cavity. The main difference between the two schemes is that the first one relies on a *resonant* interaction between the successive atoms and the field mode, while the second one is *nonresonant*.

In the scheme of Slosser and co-workers, the atom–field interaction time is chosen such that there is a number state $|N\rangle$ for which the successive atoms undergo a 6π nutation as they traverse the cavity. Such a state is called a trapping state [Filipowicz, Javanainen and Meystre 1986b, Meystre, Rempe and Walther 1988]. Also, it is assumed that the initial field density matrix is confined between the vacuum state and $|N\rangle$.

Slosser, Meystre and Wright [1990] numerically solved the micromaser field master equation [Filipowicz, Javanainen and Meystre 1986a, Bergou et al. 1989]

$$\partial\rho_{\mathrm{f}}/\partial t = L\rho_{\mathrm{f}} + R[F(\tau) - I]\rho_{\mathrm{f}}\,, \tag{8.2}$$

where I is the identity operator, under these conditions. They showed that for high enough relative injection rates N_{ex}, the field evolves to an excellent degree of approximation toward a pure state with the character of a macroscopic superposition of quantum states. Their results are summarized in figs. 4 and 5, which demonstrate how the quantitative nature of the steady-state solution changes as N_{ex} is increased. Figure 4 gives the mean photon number (solid line) as well as the Fano factor of the field (dashed line) as a function of N_{ex}. We observe a distinct transition between two final states of

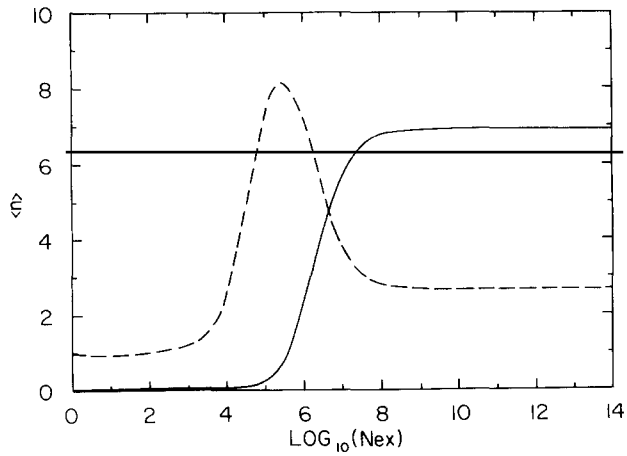

Fig. 4. Mean photon number $\langle n\rangle$ (solid curve) and Fano factor σ^2 (dashed curve) as a function of log N_{ex} for $N_{\mathrm{ex}} = 15$, $\alpha = 0.53$. (After Slosser, Meystre and Wright 1990].)

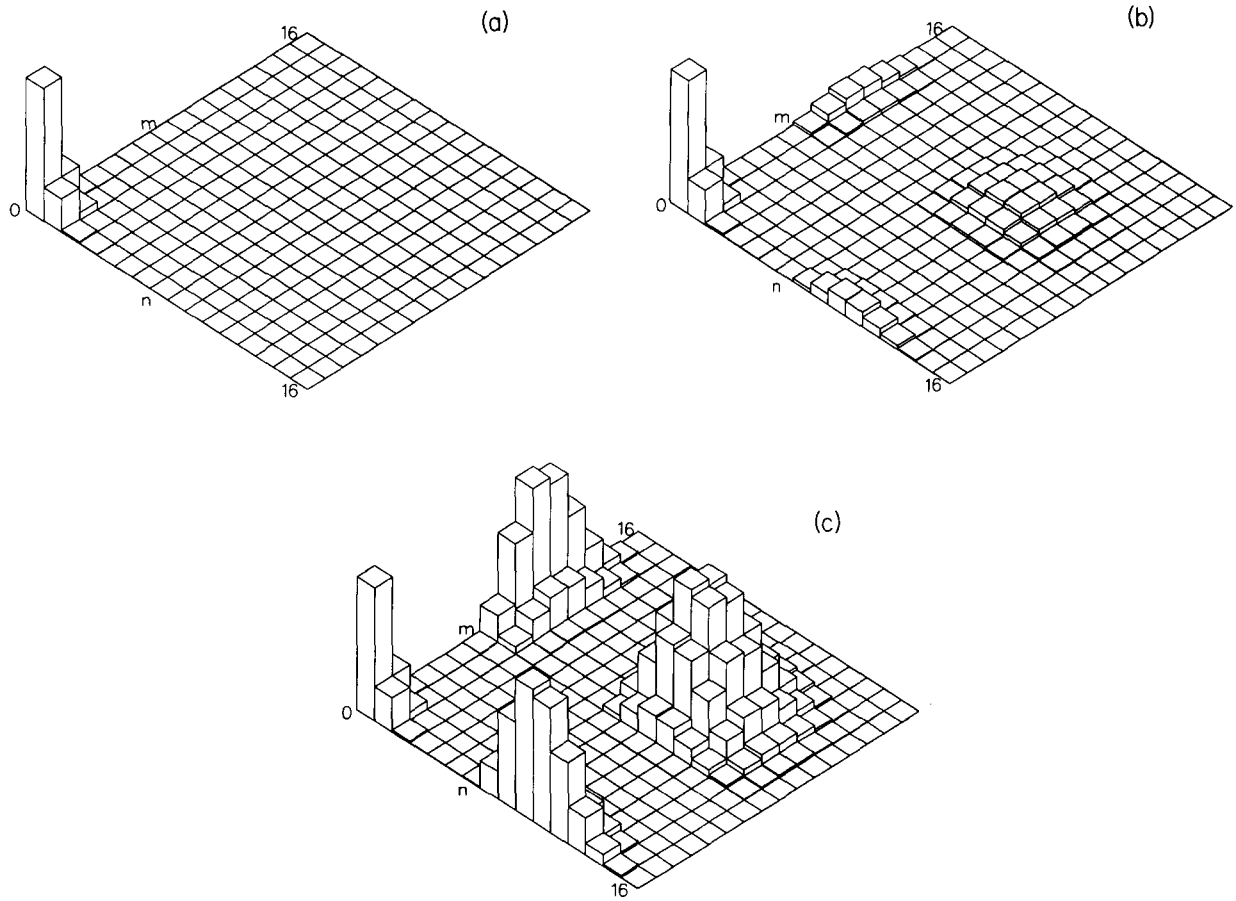

Fig. 5. Moduli of the field density matrix elements $\langle n|\rho_f|m\rangle$ for (a) $N_{ex} = 15$, (b) $N_{ex} = 10^6$ and (c) $N_{ex} = 10^9$. Here $N_u = 15$, $\alpha = 0.53$. (After Slosser, Meystre and Wright [1990].)

completely different nature, the transition region being characterized by a strong peak in field fluctuations suggestive of a phase-transition-like phenomenon. Below the transition the field is essentially poissonian (vacuum field), while it is superpoissonian above the transition region.

Figure 5 shows the moduli of the field density matrix elements $|\langle n|\rho_f|m\rangle|$ in the low-N_{ex} regime, in the transition region and in the high-N_{ex} regime. This figure clearly illustrates the transition to an almost pure "macroscopic superposition", which is given to an excellent approximation by a so-called cotangent state of the electromagnetic field [Slosser, Meystre and Braunstein 1989, Slosser and Meystre 1990].

Wilkens and Meystre [1991] have proposed a scheme to detect these macroscopic superpositions using a nonlinear version of a single-atom homodyne detector [Yuen and Shapiro 1978, Yurke 1985, Mandel 1982, Schumaker 1984, Yuen and Chan 1983, Yuen 1982, Braunstein 1990].

The nonresonant method of Brune et al. [1992] is obtained from a specialization of the QND scheme discussed in the preceding section to the case of a monokinetic atomic beam. These authors show that when applied to an initial coherent field, the measurement sequence outlined in section 6 produces quantum superpositions of coherent states of the form

$$|\psi\rangle = (|\alpha\rangle \pm |-\alpha\rangle)/\sqrt{2[1 \pm \exp(-2|\alpha|^2)]}\,, \tag{8.3}$$

provided that the atoms undergo exactly a $\pi/2$ phase shift in the two Ramsey field zones R_1 and R_2. Here, the "±" holds for exciting atoms measured in their lower or upper state, respectively. (More details are given in Haroche's contribution in this issue.) A remarkable feature of this nonresonant scheme is that if the first atom is detected, say, in the upper level $|a\rangle$, then the atoms that follow will all be detected in that same state with unit probability, provided that dissipation is neglected. The state of the field thus remains unchanged in the second and all subsequent measurement processes. In other words, a beam of atoms with appropriate velocity produces a stable Schrödinger cat of parity determined by the outcome of the first measurement. From this point of view, the non-resonant generation of macroscopic superpositions is similar to the resonant one, as the cotangent states obtained in that case leave the atom-field density matrix in a factorized form (disentangled state) at the times when the successive atoms exit the cavity [Slosser, Meystre and Braunstein 1989].

It is well-known that dissipation causes quantum coherences to be destroyed on a fast time scale. However, both the resonantly and the nonresonantly generated cats can survive the effects of coupling to the environment, provided that they are "fed" by further polarized atoms at a sufficiently high rate. In the case of resonant excitation, this leads to true steady-state cats, even if the state of the exiting atoms is not measured. This is due to the fact that the pump atoms provide both quantum coherence *and* energy to the field mode, as well as to the disentanglement of the atom–field state.

In contrast, the polarized atoms do feed quantum coherence, *but no energy*, in the nonresonant case. Hence, the monitored cats disappear after the classical field relaxation time. Note that in this case, the parity of the cat can abruptly change, as dissipation has the effect of reducing the probability that subsequent atoms are detected in the same state to slightly less than unity [Brune et al. 1992].

9. Outlook – mechanical effects

In this paper, we have sketched recent developments in cavity QED and discussed how they have and will impact our fundamental understanding of light–matter interactions in particular, and of quantum mechanics in general. Experimental progress is happening at a fast pace, and there is no doubt that many of the effects which have been proposed and reviewed here will soon be demonstrated. The question, then, is where do we go from there. We believe that an exciting new direction, which combines cavity quantum optics and "atom optics," shows considerable promise as a future theoretical and experimental playground.

Together with cavity QED, the manipulation of atomic trajectories by electromagnetic fields is one of the most exciting recent developments in quantum optics and laser spectroscopy. Here, one exploits the fact that every time an atom exchanges energy with the field, the momentum of the absorbed or emitted light must be compensated by a mechanical motion of the atom. This leads to atomic trapping and cooling, state-selective atomic reflection and diffraction by light fields, atom interferometry, etc. In these situations, it is usually sufficient to describe the fields classically, while spontaneous emission is treated as a stochastic process. In cavity QED, in contrast, the mode structure of the field as well as its quantum nature are essential.

Recently, there has been a growing effort to merge these two areas of research [Meystre, Schumacher and Stenholm 1989, Englert et al. 1991, Haroche, Brune and Raimond 1991, Wilkens, Białynicka-Birula and Meystre 1992]. Questions of particular interest are related to the effects of the internal degrees of freedom of the field (photon statistics) and of the atoms on the mechanical motion,

and also to the confinement of an atom inside a high-Q cavity, possibly in a state close to the vacuum state.

If this can be achieved, it will then be possible to investigate a fundamental quantum system consisting of a single atom coupled to a single mode of the electromagnetic field by just one quantum of excitation and bound in space by the quantum correlations between these two subsystems.

Acknowledgments

This work is supported by the US Office of Naval Research contract N00014-91-J205, by the National Science Foundation Grants PHY-8902548 and INT-8712254, and by the Joint Services Optics Program.

References

Baltes, H.P., R. Muri and F.K. Kneubühl [1970] Proc. XX PIB-Symposium, New York, p. 667.
Baltes, H.P. and Hilf E.R. [1976] Spectra of Finite Systems (Bibliographisches Institut, Mannheim).
Baltes, H.P. and F.K. Kneubühl [1972] Helv. Phys. Acta 45, 481.
Barnett, S.M. and P.L. Knight [1985] Phys. Rev. A 33, 2444.
Barnett, S.M., P. Filipowicz, J. Javanainen, P.L. Knight and P. Meystre [1986], in: Frontiers in Quantum Optics, eds E.R. Pike and S. Sarkar (Hilger, Bristol).
Bergou, J., L. Davidovich, M. Orszag, C. Benhert, M. Hillery and M.O. Scully [1989] Optics Comm. 72, 82.
Braginsky, V.B., Y.I. Vorontsov and F.Y. Khalili [1977] Sov. Phys. JETP 46, 705.
Braunstein, S.L. [1990] Phys. Rev. A 42, 474.
Brecha, R.J., L.A. Orozco, M.G. Raizen, M. Xiao and H.J. Kimble [1986] J. Opt. Soc. Am. B 3, 238.
Brune, M., J.M. Raimond and S. Haroche [1987] Phys. Rev. A 35, 154.
Brune, M., J.M. Raimond, P. Goy, L. Davidovich and S. Haroche [1987] Phys. Rev. Lett. 59, 1899.
Brune, M., S. Haroche, V. Lefevre, J.M. Raimond and N. Zagury [1990] Phys. Rev. Lett. 65, 976.
Brune, M., S. Haroche, J.M. Raimond, L. Davidovich and N. Zagury [1992] Phys. Rev. A 45, 5193.
Caldeira, A.O. and A.J. Leggett [1985] Phys. Rev. A 31, 1059.
Carmichael, H.J., R.J. Brecha, M.G. Raizen, H.J. Kimble and P.R. Rice [1989] Phys. Rev. A 40, 5516.
Caves, C.M. [1983] in: Quantum Optics, Experimental Gravitation and Measurement Theory, eds P. Meystre and M.O. Scully (Plenum Press, New York) p. 567.
Caves, C.M., K.S. Thorne, R.W.P. Drever, V.D. Sandberg and M. Zimmerman [1980] Rev. Mod. Phys. 52, 341.
Cohen-Tannoudji, C. and J. Dalibard [1986] Europhys. Lett. 1, 441.
Cook, R.J. and H.J. Kimble [1985] Phys. Rev. Lett. 54, 1023.
Cook, R.J. and P.W. Milonni [1987] Phys. Rev. A 35, 5081.
Cummings, F.W. [1965] Phys. Rev. 140, A1051.
Davidovich, L., J.M. Raimond, M. Brune and S. Haroche [1987] Phys. Rev. A 36, 3771.
Dehmelt, H. [1975] Bull. Am. Phys. Soc. 20, 60.
Eberly, J.H., N.B. Narozhny and J.J. Sanchez-Mondragon [1980] Phys. Rev. Lett. 44, 1323.
Englert, B.G., J. Schwinger, A.O. Barut and M.O. Scully [1991] Europhys. Lett. 14, 25.
Filipowicz, P., J. Javanainen and P. Meystre [1986a] Phys. Rev. A 34, 3077.
Filipowicz, P., J. Javanainen and P. Meystre [1986b] J. Opt. Soc. Am. B 3, 906.
Haroche, S. [1982] in: New Trends in Atomic Physics, Vol. 1, eds G. Grynberg and R. Stora (North-Holland, Amsterdam).
Haroche, S. [1992] in: Fundamental Systems in Quantum Optics, eds J. Dalibard, J.M. Raimond and J. Zinn-Justin (Elsevier, Amsterdam).
Haroche, S. and J.M. Raimond [1985] in: Advances in Atomic and Molecular Physics, Vol. 20, eds D. Bates and B. Bederson (Academic Press, New York).
Haroche, S., M. Brune and J.M. Raimond [1991] Europhys. Lett. 14, 19.
Heinzen, D.J., J.J. Childs, J.E. Thomas and M.S. Feld [1987] Phys. Rev. Lett. 58, 1320.
Imoto, N. and S. Saito [1989] Phys. Rev. A 39, 675.
Imoto, N., H.A. Haus and Y. Yamamoto [1985] Phys. Rev. A 32, 2287.
Imoto, N., S. Watkins and Y. Sasaki [1987] Optics Comm. 61, 159.
Javanainen, J. [1986] Phys. Rev. A 33, 2121.
Jaynes, E.T. and F.W. Cummings [1963] Proc. IEEE 51, 89.
Kaluzny, Y., P. Goy, M. Gross, J.M. Raimond and S. Haroche [1983] Phys. Rev. Lett. 51, 1175.

Kimble, H.J. [1990] private communication.
Kleppner, D. [1981] Phys. Rev. Lett. 47, 233.
Krause, J., M.O. Scully and H. Walther [1987] Phys. Rev. A 36, 4547.
Kruase, J., M.O. Scully, T. Walther and H. Walther [1989] Phys. Rev. A 39, 1915.
Lamb Jr., W.E. [1985] in: Chaotic Behaviour of Quantum Systems, Theory and Applications, ed. G. Casati (Plenum Press, New York).
Lamb Jr., W.E. [1986] in: New Techniques and Ideas in Quantum Measurement Theory, ed. D.M. Greenberger, Ann. New York Acad. Sci. Vol. 480 (The New York Academy of Sciences, New York).
Leggett, A.J. [1980] Prog. Theor. Phys. Suppl. 69, 80.
Louisell, W.H. [1990] Quantum Statistical Properties of Radiation (Wiley, New York).
Lugiato, L., M.O. Scully and H. Walther [1987] Phys. Rev. A 36, 740.
Mandel, L. [1982] Phys. Rev. Lett. 49, 136.
Martinis, J.M., M.H. Devoret and J. Clarke [1988] Phys. Rev. B 35, 4682.
Meschede, D. [1992] Phys. Rep. 211, 201.
Meschede, D., H. Walther and G. Müller [1985] Phys. Rev. Lett. 54, 551.
Meystre, P. [1987] Opt. Lett. 12, 669.
Meystre, P. [1989] in: Squeezed and Nonclassical Light, eds P. Tombesi and E.R. Pike (Plenum Press, New York).
Meystre, P. [1992] in: Progress in Optics, Vol. 30, ed. E. Wolf (North-Holland, Amsterdam), in press.
Meystre, P. and M. Sargent III [1991] Elements of Quantum Optics, 2nd Ed. (Springer, Berlin).
Meystre, P. and E.M. Wright [1988] Phys. Rev. A 37, 2524.
Meystre, P., A. Quattropani and H.P. Baltes [1974] Phys. Lett. A 49, 85.
Meystre, P., A. Quattropani, A. Faist and E. Geneux [1975] Nuovo Cimento 25, 521.
Meystre, P., G. Rempe and H. Walther [1988] Opt. Lett. 13, 1078.
Meystre, P., E. Schumacher and S. Stenholm [1989] Optics Comm. 73, 443.
Meystre, P., J.J. Slosser and M. Wilkens [1990] Optics Comm. 79, 300.
Milonni, P.W. and P.L. Knight [1973] Optics Comm. 9, 119.
Nagourney, W., J. Sandberg and H. Dehmelt [1986] Phys. Rev. Lett. 56, 2727.
Nayak, N., R.K. Bullough and B.V. Thompson [1990] in: Coherence and Quantum Optics. VI, eds J.H. Eberly, L. Mandel and E. Wolf (Plenum Press, New York).
Ogawa, T., M. Ueda and N. Imoto [1991] Phys. Rev. Lett. 66, 1046.
Parker, J. and C.R. Stroud [1987] Phys. Rev. A 35, 4226.
Purcell, E.M. [1946] Phys. Rev. 69, 681.
Raizen, M.R., R.J. Thompson, R.J. Brecha, H.J. Kimble and H.J. Carmichael [1989] Phys. Rev. Lett. 63, 240.
Ramsey, N.F. [1985] Molecular Beams (Oxford Univ. Press, Oxford).
Rempe, G., H. Walther and N. Klein [1987] Phys. Rev. Lett. 58, 353.
Rempe, G., F. Schmidt-Kaler and H. Walther [1990] Phys. Rev. Lett. 64, 2483.
Savage, C.M. [1990] Quantum Opt. 2, 89.
Savage, C.M. and D.F. Walls [1985] Phys. Rev. A 32, 2316.
Schenzle, A., R.G. deVoe and R.G. Brewer [1986] Phys. Rev. A 33, 2127.
Schumaker, B.L. [1984] Opt. Lett. 9, 189.
Slosser, J.J. and P. Meystre [1990] Phys. Rev. A 41, 3867.
Slosser, J.J., P. Meystre and S.L. Braunstein [1989] Phys. Rev. Lett. 63, 934.
Slosser, J.J., P. Meystre and E.M. Wright [1990] Opt. Lett. 15, 233.
Srinivas, M.D. and E.B. Davies [1981] Opt. Acta 28, 981.
Srinivas, M.D. and E.B. Davies [1982] Opt. Acta 29, 235.
Thorne, K.S., C.M. Caves, V.D. Sandberg, M. Zimmerman and R.W.P. Drever [1979] in: Sources of Gravitational Radiation, ed. L. Smarr (Cambridge Univ. Press, Cambridge) p. 49.
Ueda, M. [1989] Quantum Opt. 1, 131.
Ueda, M., N. Imoto and T. Ogawa [1990] Phys. Rev. A 41, 3891.
Unruh, W.G. [1987] Phys. Rev. D 18, 1764.
Walls, D.F. and G.J. Milburn [1985] Phys. Rev. A 31, 2403.
Weisskopf, V. and E. Wigner [1930] Z. Phys. 63, 54.
Wilkens, M. and P. Meystre [1991] Phys. Rev. A 43, 3832.
Wilkens M., Z. Białynicka-Birula and P. Meystre [1992] Phys. Rev. A 45, 477
Wright, E.M. and P. Meystre [1988] Opt. Lett. 14, 177.
Yuen, H.P. [1982] Phys. Lett. A 91, 101.
Yuen, H.P. and V.W.S. Chan [1983] Opt. Lett. 8, 177.
Yuen, H.P. and J.H. Shapiro [1978] IEEE Trans. Int. Theory 24, 657.
Yurke, B. [1985] Phys. Rev. A 32, 311.
Yurke, B. and D. Stoler [1986] Rev. Lett. 57, 13.